Talanta 130 (2014) 33–38

Contents lists available at ScienceDirect

Talanta

journal homepage: www.elsevier.com/locate/talanta

# Enzyme-free amplification for sensitive electrochemical detection of DNA via target-catalyzed hairpin assembly assisted current change

Yong Qian [a], Chunyan Wang [a], Fenglei Gao [b,*]

[a] Fundamental Science on Radioactive Geology and Exploration Technology Laboratory, East China Institute of Technology, Nanchang 330013, Jiangxi, China
[b] Jiangsu Key Laboratory of Target Drug and Clinical Application, School of Pharmacy, Xuzhou Medical College, 221004 Xuzhou, China

ARTICLE INFO

*Article history:*
Received 5 April 2014
Received in revised form
18 June 2014
Accepted 22 June 2014
Available online 30 June 2014

*Keywords:*
Enzyme-free
Signal amplification
Electrochemical
Sensors

ABSTRACT

An isothermal, enzyme-free and sensitive method for electrochemical detection of DNA is proposed based on target catalyzed hairpin assembly and for signal amplification. Molecular beacon 1 (MB1) contains a ferrocene (Fc) tag, which was immobilized on the gold electrode as recognition probe to hybridize with target DNA. Then, molecular beacon 2 hybridized with the opened MB1, allowing the target to be displaced. The displaced target again triggered the next round of strand exchange reaction resulting in many Fc far away from the GE to achieve signal amplification for sensitive DNA detection. The current signal amplification strategy is relatively simple and inexpensive owing to avoid the use of any kind of enzyme or sophisticated equipment. It can achieve a sensitivity of 42 fM with a wide linear dynamic range from $10^{-13}$ to $10^{-9}$ M and discriminate mismatched DNA from perfect matched target DNA with a high selectivity. The proposed method showed excellent specificity, high sensitivity and low detection limit, and could be applied in analysis of real samples.



## 1. Introduction

Rapid, simple and sensitive determination of sequence-specific DNA has become increasingly important in clinical diagnosis, food analysis and bioterrorism/environmental monitoring over the past few years [1–4]. Great efforts have been made to develop the more sensitive methods for the detection of DNA with the aim of making portable and affordable devices. Various sensitive detection modes including fluorescence [5,6], chemiluminescence [7], colorimetry [8,9] surface-enhanced Raman scattering [10,11] electric signal [12] and electrochemical techniques [13–15] have been used for detecting and quantifying sequence-specific DNA. Among the various biosensing approaches available to date, electrochemical sensing appears to be one of the most promising approaches due to the rapid and sensitive response, low fabrication cost and operational convenience [16–19]. Despite its significant advantages, the traditional electrochemical DNA sensor is not sensitive enough because of that a single target molecule only reacts with a single signaling probe, limiting the total signal gain and corresponding sensitivity. Therefore, there is still a great desire to improve the performance of electrochemical DNA sensors in sensitivity.

DNA recycling, wherein signal amplification is achieved by allowing a single DNA target molecule to interact with multiple nucleic acid-based signaling probes, represents an interesting alternative [20–22]. In this approach, target-probe hybridization catalyzes the selective enzymatic digestion of the signaling probe, releasing the intact DNA target to initiate the digestion of other probe molecules, thereby generating multiple signaling events and achieving signal amplification. This approach has previously been demonstrated using nuclease, e.g., endonuclease, polymerase, and exonuclease [23–25]. However, the protein enzymes needed in these approaches are expensive, which increase the detection cost and may limit the application of these techniques. For example, the polymerase-based methods require the addition of dNTPs and thus a complex polymerase replication process. Therefore, the enzyme-free DNA biosensor fabrication with superior detection sensitivity is highly desirable. Recently, some enzyme-free methods have attracted growing interests for amplification detection of DNA, such as hybridization chain reaction [26], entropy-driven catalysis [27], and target-catalyzed hairpin assembly [28,29]. However, only a few works developed for DNA detection by target catalyzed hairpin assembly are mainly operated by fluorescent signal readouts [30]. Herein, we reported a novel electrochemical method for DNA detection via target-catalyzed hairpin assembly assisted current change. The detailed concept of strategy is illustrated in Scheme 1.

Molecular beacon 1 (MB1) contains a thiol group at the 5′ end and a ferrocene (Fc) tag at the 3′ end, which was immobilized on

* Corresponding author. Tel./fax: +86 516 83262138.
*E-mail address:* jsxzgfl@sina.com (F. Gao).

http://dx.doi.org/10.1016/j.talanta.2014.06.051
0039-9140/

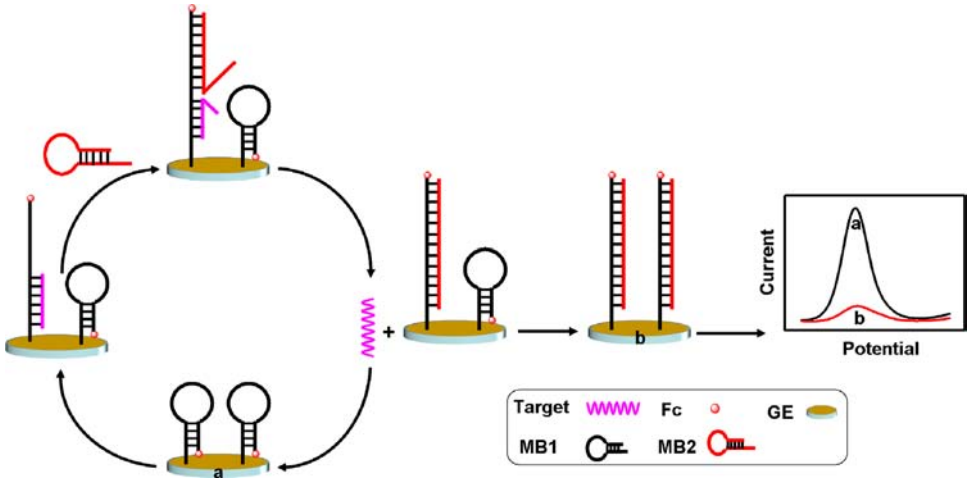


**Scheme 1.** Schematic illustration of enzyme free amplification strategy for electrochemical DNA detection via target-catalyzed hairpin assembly assisted current change.

the gold electrode (GE) as recognition probe. Differential pulse voltammetry (DPV) was used for the investigation of the electrochemical oxidation signal of the covalently attached Fc on the MB probes, because DPV is a pulse technique that possesses higher sensitivity than conventional sweep techniques. In the absence of target DNA, MB1 was not opened, so the Fc group close to the surface of GE due to the formation of a hairpin-like conformation and results in a high oxidation signal being observed. However, when target DNA hybridizes to the MB1, MB1 was opened and assembled with molecular beacon 2 (MB2) to displace the target DNA, which becomes available for the next cycle of MB1-target hybridization. Eventually, each target strand can go through many cycles, resulting in many Fc far away from the GE. As a result, the peak current of Fc dramatically decreases. Electrochemical impedance spectroscopy (EIS) and polyacrylamide gel electrophoresis (PAGE) were also used to study the process of target-catalyzed hairpin assembly. The proposed strategy showed high sensitivity and selectivity toward DNA detection, which provides a useful platform for bioanalytical and clinic biomedical application.

## 2. Experimental

### 2.1. Oligonucleotides and regents

All other chemicals used in this work were of analytical grade. Water was purified with a Milli-Q purification system (Branstead, USA) and used throughout the work. The buffers used in the study were HEPES buffer (10 mM HEPES, 150 mM NaCl, pH 7.4) for target binding, The washing buffer was PBS (50 mM $Na_2HPO_4$, 50 mM $NaH_2PO_4$, 1 M NaCl, pH 7.5). To avoid the instability of ferrocenium (the oxidized form of the ferrocene), 1.0 M $NaClO_4$ solution was used as the supporting electrolyte when electrochemical behavior of the working electrode was investigated. DNA oligonucleotides used in this work were synthesized and purified by Takara Biotechnology Co., Ltd. (Dalian, China).

MB1: 5′-SH-AAGTAGTGATTGAGCGTGATGAATGTCACTACTTCAA-CTCGCATTCATCACGCTCAATC-Fc-3′

MB2: 5′-TGATGAATGCGAGTTGAAGTAGTGACATTCATCACGCTC-AATCACTACTTCAACTCGCA-3′

Target: 5′-GACATTCATCACGCTCAATCACTACTT-3′

Single-base mismatched: 5′-GACATTCATCACACTCAATCACTACTT-3′

Non-complementary: 5′-ATGCTGACTGACAAGCTTAGCAAGGG-3′

### 2.2. Electrode modification

Prior to modification, the bare GE (3 mm in diameter) was polished to a mirror-like surface with alumina suspensions and then sequentially cleaned ultrasonically in 95% ethanol and twice-quartz-distilled water for 5 min. Prior to attachment to the gold surface, thiolated MB1 was incubated with 100 mM TCEP for 1 h to reduce disulfide bonds and subsequently diluted to 1.0 μM with phosphate buffer. The clean gold electrodes were incubated in this reduced probe solution for 6 h at room temperature in the dark. The probe-functionalized surface was subsequently passivated with 6 mM 6-mercaptohexanol for 2 h at room temperature. The electrodes were rinsed with DI water and stored in phosphate buffer for at least 1 h to equilibrate the probe structures prior to electrochemical measurements. 5 μL target DNA with the designed concentration and 5 μL MB2 (300 nM) were dropped on the surface of the electrodes. After the process was performed for 2 h at 37 °C, it was terminated by washing thoroughly. All process takes 12 h to complete the modification. The whole procedure was shown in Scheme 1.

### 2.3. Measurement procedure

Electrochemical experiments were carried out using the CHI 660C electrochemical analyzer. Cyclic voltammetry (CV) results were recorded within a potential range of 0 to 0.6 V (scan rate-$=0.05\ V\ s^{-1}$). For all measurements, 4 successive cycles were carried out to ensure signal stabilization and the fourth cycle was kept as the result. Differential pulse voltammograms (DPVs) of Fc tag were registered in the potential interval 0.0 to +0.6 V vs. Ag/AgCl under the following conditions: modulation amplitude 0.05 V, pulse width 0.06 s, and sample width 0.02 s. The EIS measurement was also carried out with the CHI 660C electrochemical analyzer. Supporting electrolyte solution was 1.0 mmol $L^{-1}$ $K_3[Fe(CN)_6]/K_4[Fe(CN)_6]$ (1:1) solution containing 0.1 mol $L^{-1}$ KCl. The ac voltage amplitude was 5 mV, and the voltage frequencies used for EIS measurements ranged from 100 kHz to 100 mHz. The applied potential was 172 mV vs. Ag/AgCl.

### 2.4. Gel electrophoresis

A 20% non-denaturing PAGE analysis of the products was carried out in 1 × TBE (pH=8.3) at 80 V constant voltage for about 3 h. After Sybr green I staining, gels were scanned using an Image Master VDS-CL (Amersham Biosciences).

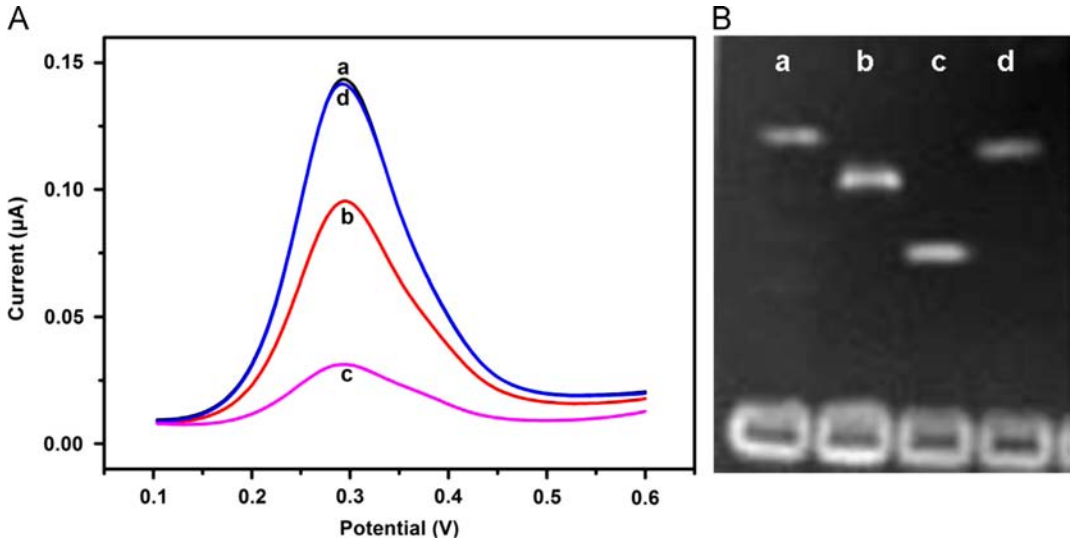


**Fig. 1.** (A) DPVs curves for the sensor in the presence of (*a*) blank, (*b*) 1 nM target, (*c*) 1 nM target, and 0.3 μM MB2, (*d*) 0.3 μM MB2 and (B) PAGE analysis of (a) 0.1 μM MB1, (b) 0.1 μM MB1, and 0.1 μM target, (c) 0.1 μM MB1, 0.1 μM MB2 and 0.1 μM target for 2 h, (d) 0.1 μM MB1 and 0.1 μM MB2.

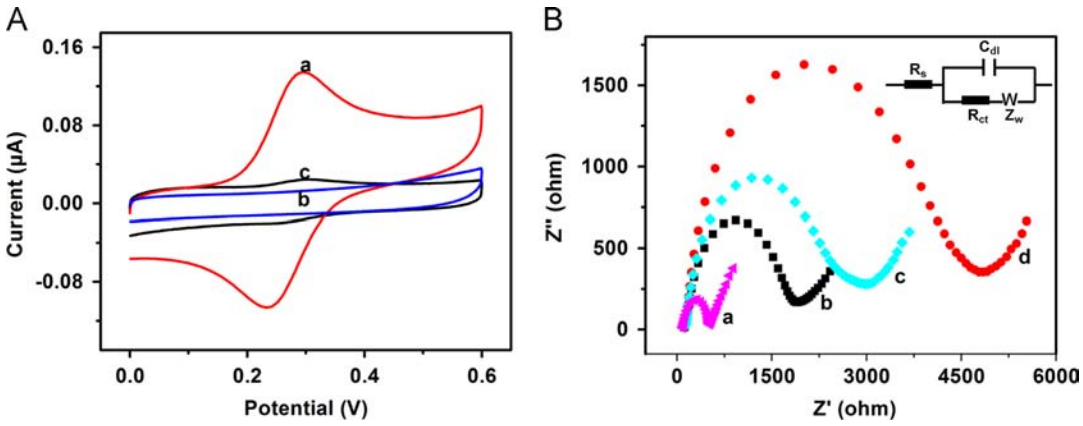


**Fig. 2.** (A) CV curves of (*a*) the electrode immobilized with MB1, (*b*) bare GE, and (*c*) after the hybridization of MB1 and target sequences (scan rate 0.05 V $s^{-1}$). The electrolyte is 1 M $NaClO_4$. (B) EIS spectroscopy during the progress of (*a*) bare gold electrode, (*b*) the electrode immobilized with MB1; (*c*) after the hybridization of MB1 and target sequences; (*d*) after the hybridization of MB1 and target sequences in the presence of MB2 for 2 h. Inset: standard Randles circuit.

## 3. Results and discussion

### 3.1. Verification of the amplified DNA detection method

To demonstrate the feasibility of this strategy, the electrochemical behavior of Fc at different sensing interfaces was investigated, and the results are shown in Fig. 1A. In the absence of target DNA, the stem-loop structure of the hairpin probe held the Fc tag in close proximity with the electrode surface, thus ensuring rapid electron transfer and efficient Fc oxidation (curve *a*). Consequentially, a significant signal was achieved. After the addition of the target DNA, a change in redox currents was observed. This was because the Fc label was separated from the electrode surface (curve *b*). Furthermore, in the MB2 assisted system, it was found that the intensity of the current sharply decreased after the MB2 was added (curve *c*), compared with the conventional method, which employs MB1 only, the MB2-aided amplification method led to a 3-fold decrease in the signal intensity after 2 h. Clearly, the signal enhancement was caused by the cycling use of the target DNA and the continuous generation of the MB1–MB2 complex as shown in Fig. 1A. For the solution containing MB2 only, the current intensity remained nearly unchanged (curve *d*), indicating that the hairpin structures of MB2 could not open the loop of MB1. Therefore, the target-catalyzed hairpin assembly-related DNA recycling produced a highly sensitive method for the detection of DNA.

PAGE analysis was also used to investigate the viability of the sensing strategy (Fig. 1B). Probe 1 exhibited only one band (lane a). After target was added in the solution, a new band appeared (lane b), which corresponded to the formed double stranded DNA. After MB was further added to the mixture, a new product band with a slow migration speed was observed (lane c). This result should be contributed to the product of MB1-target-MB2, verifying target-catalyzed hairpin process. As shown in Fig. 1B, when mixing the MB1 and MB2, there was almost no MB1-MB2 complex formed (lane d). This phenomenon indicated that the two stable MB1 and MB2 can coexist in solution.

### 3.2. Characterization of DNA sensors

The interface properties of surface-modified electrodes were investigated by CV and EIS measurements. The CV of the different modification steps have been shown in Fig. 2. In the absence of target DNA, an Fc redox peak pair at 0.241 and 0.294 V is observed with the MB-modified gold electrodes (Fig. 2A, curve *a*). We thus ascribe this peak pair to the redox conversion of Fc labels in close

proximity to the gold electrode. Bare gold electrodes, in contrast, do not produce CV peaks in the relevant potential range (curve *b*). While in the presence of high target DNA concentration, the couple of redox peaks almost disappeared (curve *c*). Those observations implied that the redox process takes place only from the surface and this biosensor was sensitively responsive to target DNA.

EIS is a powerful tool for investigating the interfacial properties of surface-modified electrode. The typical electrochemical interface can be represented as an electrical circuit as shown in the inset of Fig. 2B (Randles and Ershler theoretical model [31]). The equivalent circuit includes four parameters. The ohmic resistance of the electrolyte solution, $R_s$, the Warburg impedance, $Z_w$, represent bulk properties of the electrolyte solution and diffusion features of the redox probe in solution. The double-layer capacitance, $C_{dl}$, and the charge-transfer resistance, $R_{ct}$, reveal interfacial properties of the electrode, which is highly sensitive to the surface modification. Usually, $R_{ct}$ controls the interfacial electron-transfer rate of the redox probe between the solution and the electrode. In the Nyquist plot of impedance spectroscopy, $R_{ct}$ at the electrode surface is equal to the semicircle diameter. Fitting of the equivalent circuit to the experimental data yielded the solid lines drawn in Fig. 2B. The bare GE has a relatively low resistance with a small semicircle domain (curve *a*), when the capture probe is assembled onto the electrode surface, the semicircle increases remarkably, owing to negatively charged interface electrostatically repelled the negatively charged $[Fe(CN)_6]^{3-/4-}$ redox probe and inhibited interfacial charge transfer (curve *b*). After the target DNA was hybridized with MB1, $R_{ct}$ further increased (curve *c*). After hybridization, there were more negative charges on the surface and the DNA modified layer became thicker. These two factors led to the further increase of $R_{ct}$ value [32–34]. The $R_{ct}$ largely increased when MB2 were attached to due to the cycling use of the target DNA and the continuous generation many of the MB1–MB2 complex (curve *d*). In addition, the $C_{dl}$ values deduced for a standard Randles circuit is $C_{dl}=(\omega_0 R_{ct})^{-1}$($Z_{im}$: the imaginary component of impedance; $\omega_0$: the $\omega$ where $Z_{im}$ in the semicircle is maximum and equals $R_{ct}/2$) [35]. According to the equation, we can deduce that the trend of the capacity is decreased due to the increased trend of $R_{ct}$ during each modification.

### 3.3. Optimization of experimental conditions

The reaction conditions play an important role in the sensing process, such as the MB2 concentration and the incubation time. In order to achieve the best signal-to-noise level, the reaction conditions were optimized. To investigate the effect of the concentration of MB2 on the detection system, target DNA (0.1 nM) was mixed with MB2 at different concentrations ranging from 0 to 400 nM. As shown in Fig. 3A, the current intensity of the system decreased as the concentration of MB2 increased. Furthermore, the optimum concentration of MB2 used in this system was 300 nM due to its best signal-to-noise level. As shown in Fig. 3B, it could be found that the electrochemical signal decreased with the reaction time before reaching saturation after 2 h, indicating strongly that target DNA could go through many cycles to open the MB1. Considering this issue, 2 h was chosen as the reaction time. It is seen that the signal of the sensing system decreased with increase of the concentration of MB2 and time in the absence of the target DNA. This background signal was due to the hybridization of MB1 with MB2. Fortunately, the decrement was less than about 6%, and upon the addition of the target DNA, the current signal of the sensing system was significantly smaller than the control. Surface density of hairpins MB on the electrode is a key factor influencing the analytical properties of the sensor. Every MB probe has been modified an Fc tag, so surface density is proportional to the electrochemical signal of Fc. In order to achieve the best surface density, we investigate the effect of the immobilization time on the electrochemical signal. As indicated from Fig. 3C, the current intensity increased with the increasing incubation time, and tended to level off after 6 h. To achieve the best surface density, 6 h was selected as the optimal deposition time.

### 3.4. Sensitivity of the electrochemical DNA biosensor

Under the optimal assay conditions, the sensitivity of the electrochemical DNA biosensor for the detection of the target DNA was investigated by varying the target DNA concentration. As shown in Fig. 4, the current decreased with the increasing target DNA concentration, and the dose–response curve showed a liner range from $10^{-13}$ to $10^{-9}$ M. The regression equation was $I$ (μA)= −0.0299 Log $c$ (mol $L^{-1}$)–0.2207 ($R^2$=0.9893), where $I$ was the current intensity subtracting the background signal and $c$ was the target DNA concentration. The detection limit of 42 fM could be estimated by using $3\sigma$, compared to the existing electrochemical methods based on the conformational change of the redox-labeled probe strategies [36] (10 pM), the proposed method can get a lower detection limit and has a higher sensitivity.

To confirm that the high sensitivity of the current strategy was the consequence of the target-induced circular reactions between the MBs and target, control experiments involving MB1 only at different target concentrations were conducted at similar conditions. As shown in Fig. 5, the current intensity decreased with the increasing concentration of target in the range from $10^{-11}$ to $10^{-7}$ mol $L^{-1}$. The correlation equation was $I$ (μA)= −0.03063 Log $c$ (mol $L^{-1}$)−0.19793 ($R^2$=0.9884). The detection limit was 3.5 pmol $L^{-1}$ from three times the standard deviation corresponding to the blank sample detection [37], which were about 100 times higher than that obtained in the presence of MB2. At the same target concentrations of 0.1 and 10 nmol $L^{-1}$, the current intensity in the presence of MB2 was 1.43 and 1.54 times higher than that in the absence of MB2, respectively. Thus the high sensitivity of this method was mainly attributed to the amplification of target-catalyzed hairpin assembly process, which made many of Fc separate from the surface of GE.

### 3.5. Selectivity of the electrochemical DNA biosensor

To investigate the specificity of the sensing system, we compared the electrochemical response induced by DNA strands containing single-base and non-complementary oligonucleotides with that of target DNA at concentrations of 10 pmol $L^{-1}$. A comparison of the three responses and background is shown in Fig. 6, the single-base mismatch sequence showed a response 1.84 times higher than that of the perfectly complementary target, while the responses to the non-complementary strand and the background were further higher than that of the single-base mismatch sequence, indicating good selectivity for the sequence detection of target DNA. This high specificity arose from the specific recognition of MB for target and the conformational constraint of the stem-loop structure of MB. These results demonstrate that this proposed method is able to detect the target effectively with high specificity, and has great potential for single nucleotide polymorphism analysis.

### 3.6. Reproducibility for target DNA detection

The reproducibility of the biosensor was an important factor of biosensor. The reproducibility of the suggested electrochemical detection method was examined by five repetitive measurements of 10 pM target DNA on a single electrode, which showed a relative

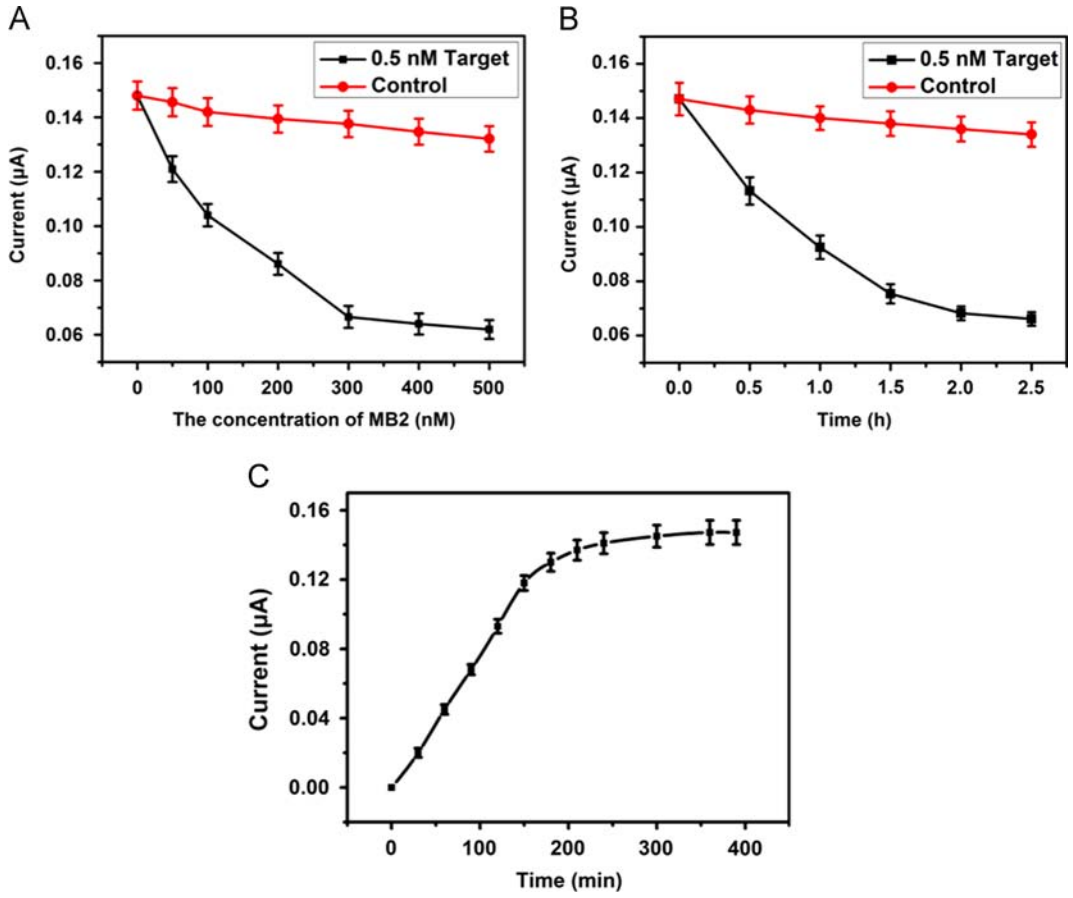


**Fig. 3.** Effect of (A) the amount of MB2 and (B) assembly time on the signal-to-noise level of the detection system. The dots represent the current intensity in the absence of Target1 (red dots) or in the presence of target (10 pM) (black squares), respectively. (C) The assembly time of MB1. When one parameter changes the others are under their optimal conditions ($n=3$). (For interpretation of the references to color in this figure legend, the reader is referred to the web version of this article.)

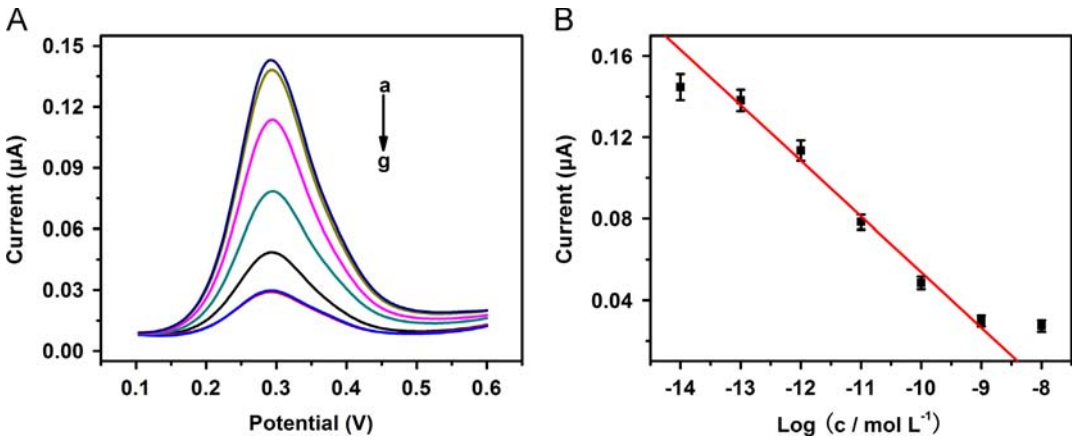


**Fig. 4.** (A) DPV curves of Fc for detection of DNA at target DNA concentrations of $10^{-14}$–$10^{-8}$ mol $L^{-1}$ in the presence of MB2; (B) linear relationship between peak current and the logarithm of target DNA concentration ($n=3$).

standard deviation (RSD) of 3.2%. The RSD for five parallel DNA sensors were fabricated on different electrode using the same experimental conditions was 5.0%. These results indicated the satisfactory reproducibility for both DNA detection and DNA sensor fabrication.

### *3.7. Real samples assay*

To test the generality of the developed DNA sensors in the clinical sample, recovery testing was carried out by spiking target DNA solution into human serum. Two targets DNA samples including 1.0 pM and 0.1 nM were spiked into the human serum, which were assayed by the developed DNA sensors. The recoveries were 94.2 and 104.1%, respectively, implying that the methodology could be used in real sample analysis for direct detection of DNA.

## 4. Conclusion

In conclusion, we have developed a simple and enzyme-free amplified sensor based on hairpin assembly reaction and target-catalytic circuits. Due to signal amplification by target-catalytic

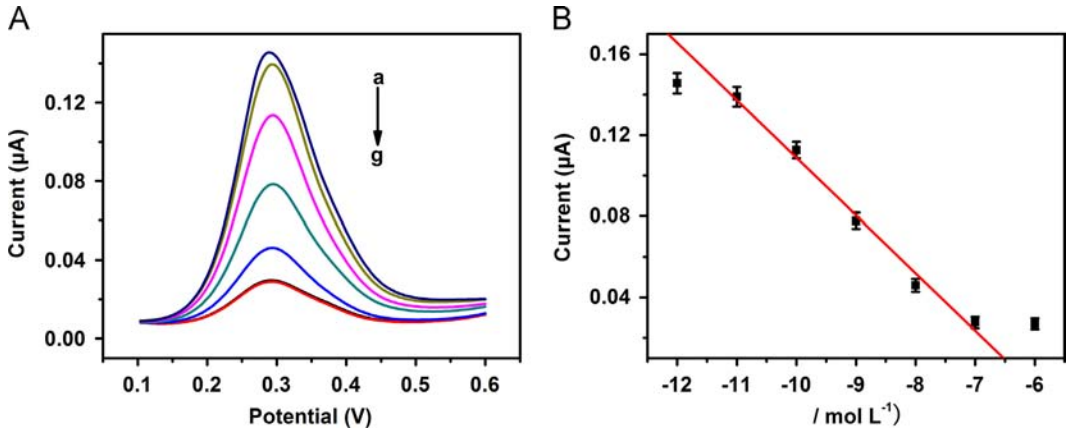


**Fig. 5.** (A) DPV curves of Fc for detection of DNA at target DNA concentrations of $10^{-12}$–$10^{-6}$ mol $L^{-1}$ in the absence of MB2; (B) linear relationship between peak current and the logarithm of target DNA concentration.

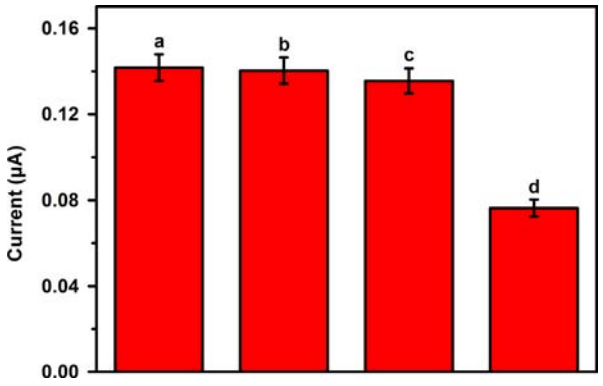


**Fig. 6.** Histograms of current intensity for (a) blank, (b) 10 pmol $L^{-1}$ single-base mismatch, (c) non-complementary sequences, and (d) complementary.

circuits, this strategy showed a detection limit down to the sub-picomolar level, which were about 2 orders of magnitude lower than that of the conventional electrochemical analysis. Furthermore, the proposed amplified sensor is enzyme-free, making it more simple and cost effective. Moreover, the approach could also be used to detect extensive targets, including proteins, small molecules, and metal ions, if the recognition molecules used can produce initiator DNA strand. Therefore, the method presented here can be expected to provide a simple, sensitive and selective platform for biomedical research and clinical diagnosis.

## Acknowledgments

This work was supported by the National Natural Science Foundation of China (nos. 21264001, 21004009), Excellent Talents of Xuzhou Medical College (D2014007), Natural Science Foundation of Jiangxi Province (20114BAB213010) and Young Scientist Foundation of Jiangxi Province (20133BCB23020).

## References

[1] A.R. Gao, N. Lu, P.F. Dai, T. Li, H. Pei, X.L. Gao, Y.B. Gong, Y.L. Wang, C.H. Fan, Nano Lett. 11 (2011) 3974–3978.
[2] E.G. Ju, X.J. Yang, Y.H. Lin, F. Pu, J.S. Ren, X.G. Qu, Chem. Commun. 48 (2012) 11662–11664.
[3] K. Hsieh, A.S. Patterson, B.S. Ferguson, K.W. Plaxco, H.T. Soh, Angew. Chem. Int. Ed. 51 (2012) 4896–4900.
[4] R.L. Stoermer, K.B. Cederquist, S.K. McFarland, M.Y. Sha, S.G. Penn, C.D. Keating, J. Am. Chem. Soc. 128 (2006) 16892–16903.
[5] W. Ren, H.M. Liu, W.X. Yang, Y.L. Fan, L. Yang, Y.C. Wang, C.H. Liu, Z.P. Li, Biosens. Bioelectron. 49 (2013) 380–386.
[6] J. Huang, Y.R. Wu, Y. Chen, Z. Zhu, X.H. Yang, C.Y. James Yang, K.M. Wang, W. H. Tan, Angew. Chem. Int. Ed. 50 (2011) 401–404.
[7] M. Luo, X. Chen, G.H. Zhou, X. Xiang, L. Chen, X.H. Ji, Z.K. He, Chem. Commun. 48 (2012) 1126–1128.
[8] M.G. Deng, D. Zhang, Y.Y. Zhou, X. Zhou, J. Am. Chem. Soc. 130 (2008) 13095–13102.
[9] L.H. Tang, Y. Liu, M.M. Ali, D.K. Kang, W.A. Zhao, J.H. Li, Anal. Chem. 84 (2012) 4711–4717.
[10] J. Hu, C.Y. Zhang, Anal. Chem. 82 (2010) 8991–8997.
[11] D.V. Lierop, K. Faulds, D. Graham, Anal. Chem. 83 (2011) 5817–5821.
[12] S. Basuray, S. Senapati, A. Aijian, A.R. Mahon, H.C. Chang, ACS Nano 3 (2009) 1823–1830.
[13] J. Wang, D.K. Xu, A.N. Kawde, R. Polsky, Anal. Chem. 73 (2001) 5576–5581.
[14] J. Xu, B.Y. Jiang, J. Su, Y. Xiang, R. Yuan, Y.Q. Chai, Chem. Commun. 48 (2012) 3309–3311.
[15] F. Xuan, X.T. Luo, I.M. Hsing, Anal. Chem. 84 (2012) 5216–5220.
[16] H. Gong, T. Zhong, L. Gao, X. Li, L. Bi, H.B. Kraatz, Anal. Chem. 81 (2009) 8639–8643.
[17] Y. Jin, X. Yao, Q. Liu, J. Li, Biosens. Bioelectron. 22 (2007) 1126–1130.
[18] R. Miranda-Castro, P. De-Los-Santos-Álvarez, M.J. Lobo-Castanon, A.J. Miranda-Ordieres, P. Tunon-Blanco, Anal. Chem. 79 (2007) 4050–4055.
[19] J. Zhang, B.P. Ting, N.R. Jana, Z.Q. Gao, J.Y. Ying, Small 5 (2009) 1414–1417.
[20] J.H. Chen, J. Zhang, Y. Guo, J. Li, F.F. Fu, H.H. Yang, G.N. Chen, Chem. Commun. 47 (2011) 8004–8006.
[21] W. Xu, X.J. Xue, T.H. Li, H.Q. Zeng, X.G. Liu, Angew. Chem. Int. Ed. 48 (2009) 6849–6852.
[22] X.L. Zuo, F. Xia, Y. Xiao, K.W. Plaxco, J. Am. Chem. Soc. 132 (2010) 1816–1818.
[23] Q.P. Guo, X.H. Yang, K.M. Wang, W.H. Tan, W. Li, H.X. Tang, H.M. Li, Nucleic Acids Res. 37 (2009) e20.
[24] R. Ren, C.C. Leng, S.S. Zhang, Chem. Commun. 46 (2010) 5758–5760.
[25] F.L. Gao, Z. Zhu, J.P. Lei, Y. Geng, H.X. Ju, Biosens. Bioelectron. 39 (2013) 199–203.
[26] Y. Chen, J. Xu, J. Su, Y. Xiang, R. Yuan, Y.Q. Chai, Anal. Chem. 84 (2012) 7750–7755.
[27] D.Y. Zhang, A.J. Turberfield, B. Yurke, E. Winfree, Science 318 (2007) 1121–1125.
[28] C.P. Ma, W.S. Wang, Z.X. Li, L.J. Cao, Q.Y. Wang, Anal. Biochem. 429 (2012) 99–102.
[29] A.X. Zheng, J. Li, J.R. Wang, X.R. Song, G.N. Chen, H.H. Yang, Chem. Commun. 48 (2012) 3112–3114.
[30] J.H. Huang, X.F. Su, Z.G. Li, Anal. Chem. 84 (2012) 5939–5943.
[31] J.E.B. Randles, Discuss. Faraday Soc 1 (1947) 11–19.
[32] C.H. Luo, H. Tang, W. Cheng, L. Yan, D.C. Zhang, H.X. Ju, S.J. Ding, Biosens. Bioelectron. 48 (2013) 132–137.
[33] Y. Huang, Y.L. Zhang, X.M. Xu, J.H. Jiang, G.L. Shen, R.Q. Yu, J. Am. Chem. Soc. 131 (2009) 2478–2480.
[34] M.A. Mehrgardi, L.E. Ahangar, Biosens. Bioelectron. 26 (2011) 4308–4313.
[35] Y. Xu, Y. Jiang, H. Cai, P.G. He, Y.Z. Fang, Anal. Chim. Acta 516 (2004) 19–27.
[36] C.H. Fan, K.W. Plaxco, A.J. Heeger, Proc. Nat. Acad. Sci. U.S.A. 100 (2003) 9134–9137.
[37] L.E. Vanatta, D.E. Coleman, J. Chromatogr. A 770 (1997) 105–114.